Low-lying electronic states of CuN calculated by MRCI method

Shu-Dong Zhang(张树东)† and Chao Liu(刘超)

Shandong Provincial Key Laboratory of Laser Polarization and Information Technology, Department of Physics, Qufu Normal University, Qufu 273165, *China*

(Received 12 April 2016; revised manuscript received 1 June 2016; published online 25 August 2016)

The high accuracy *ab initio* calculation method of multi-reference configuration interaction (MRCI) is used to compute the low-lying eight electronic states of CuN. The potential energy curves (PECs) of the $X^3\Sigma^-$, $1^3\Pi$, $2^3\Sigma^-$, $1^3\Delta$, $1^1\Delta$, $1^1\Sigma^-$, $1^1\Pi$, and $^5\Sigma^-$ in a range of $R = 0.1$ nm–0.5 nm are obtained and they are goodly asymptotes to the $Cu(^2S_g) + N(^4S_u)$ and $Cu(^2S_g) + N(^2D_u)$ dissociation limits. All the possible vibrational levels, rotational constants, and spectral constants for the six bound states of $X^3\Sigma^-$, $1^3\Pi$, $2^3\Sigma^-$, $1^1\Delta$, $1^1\Sigma^-$, and $1^1\Pi$ are obtained by solving the radial Schrödinger equation of nuclear motion with the Le Roy provided Level8.0 program. Also the transition dipole moments from the ground state $X^3\Sigma^-$ to the excited states $1^3\Pi$ and $2^3\Sigma^-$ are calculated and the result indicates that the $2^3\Sigma^-$–$X^3\Sigma^-$ transition has a much higher transition dipole moment than the $1^3\Pi$–$X^3\Sigma^-$ transition even though the $1^3\Pi$ state is much lower in energy than the $2^3\Sigma^-$ state.

Keywords: CuN, electronic excited states, MRCI calculation, potential energy curves, vibrational levels, spectroscopic constants, transition dipole moment

PACS: 31.50.Bc, 31.50.Df, 31.15.vn **DOI:** 10.1088/1674-1056/25/10/103103

1. Introduction

Transition metal compounds are very important in organometallic chemistry, surface science, astrophysics, catalysis process, and others.[1–3] The knowledge of the electronic states as well as the potential energy curves (PECs) are crucial information for experimental spectroscopic studies, and they are also important for depositing the nanoscale function material films.[4] But the compounds, even though the diatomic transition-metal mononitride, are electronically complex and very difficult to treat theoretically because of the extent of electron correlation. In experiments, almost no experimental studies for CuN were conducted until recently O'Brien *et al.*[5] produced the gas phase CuN molecules by using a copper hollow cathode in a plasma discharge. Through the intracavity laser absorption spectroscopy, they observed the electronic transition spectrum of CuN in the near infrared with red-degraded bandheads at 13005, 12963, 12957, and 12948 cm^{-1}. They tentatively attributed these transitions to being due to the absorption from the $X^3\Sigma^-$ ground state of CuN. But a strong perturbation was also observed in one of the excited states. Theoretically, there are several studies devoted to predicting the electronic structures of CuN and CuN^+species.[6–9] Ferrao *et al.*[6] studied the spectroscopic properties of the ground electronic state for CuN by the CCSD(T) approach and DFT (BP86, BPW91, B3LYP) methods through using the Wachters+f basis sets for the Cu atom and aug-cc-pVTZ basis set for the N atom, and the bond distances, harmonic vibrational frequencies, dissociation energies, ionization potentials, and electron affinity were obtained. Wu[7] also studied the electronic ground state of CuN (cation, neutral, and anion) species by various DFT methods (B3LYP, BLYP, BHLYP, BPW91, and B3PW91). Xu *et al.*[8] obtained the potential energy curve for the ground state of the CuN molecule by the density function theory (B3LYP) method where the effective core basis set of LANL2DZ for Cu atom and Pople's basis set of 6-311+(d) for the N atom were used. Daoudi *et al.*[9] reported the electronic structure and bonding calculations for low-lying states of CuN and CuN^+ with CIPSI (configuration interaction by perturbation of a multiconfiguration wave function selected iteratively) method, and indicated that the ground state of CuN is $X^3\Sigma^-$ and the first low-lying excited state is $^1\Delta$ located at 1.45 eV.

However, the structure of the excited electronic states of CuN in the gas phase seems to be not well understood. In this paper, we focus on the eight low-lying electronic states of CuN, which are corresponding to the two dissociation limits $Cu(^2S_g) + N(^4S_u)$ and $Cu(^2S_g) + N(^2D_u)$, and the PECs of these states are obtained by using the multi-reference configuration interaction (MRCI) method where the Ahlrichstype basis set of def2-tzvp is selected for both Cu atom and N atom. The properties of PECs, vibrational levels, rotation constants, spectral constants, and transition dipole moments for the electronic states of CuN are discussed.

2. Computational method

The MRCI method is considered to be one of the most reliable methods of studying electronic excited states due to the electron correlation energy to be fully considered in calculations. In this paper, the ORCA program package[10] is used for the PEC calculations as in our calculations of

†Corresponding author. E-mail: zhangsd2@126.com

© 2016 Chinese Physical Society and IOP Publishing Ltd

BeCl[11] and CuC.[12] The reference wave functions for the multireference calculations are of the state-averages complete active space self-consistent field (CASSCF) type.[13,14] The Ahlrichs triple-zeta valence with new polarization function basis set def2-TZVP[15] is used for both transition metal atom Cu and the ligand atom N, where the {17s11p7d1f} atomic orbitals of the Cu atom are contracted to {6s4p4d1f} pattern {842111/6311/4111/1}, and the {11s6p2d1f} orbitals of the N atom are contracted to {5s3p2d1f} pattern {62111/411/11/1}. The final total number of contracted basis functions is 76.

Our calculations focus on the low-lying electronic states which correspond to the dissociation limits $Cu(^2S_g)+N(^4S_u)$ and $Cu(^2S_g)+N(^2D_u)$, where the Cu keeps in the ground state ^2S_g. The ratio of the expectation values of the 4s and 3d radii of Cu is $\langle r_{4s}\rangle/\langle r_{3d}\rangle \approx 3.4$ at the Hartree–Fock numerical level,[16] and the Hartree–Fock energy levels of 3d and 4s orbital of Cu are (−13.32) eV and (−6.54) eV. Considering the dissociation limits of $Cu(^2S_g)+N(^4S_u)$ and $Cu(^2S_g)+N(^2D_u)$ to be little related to the 3d electron of Cu, it is appropriate to choose only the $4s^1$ electron of Cu and the $2s^22p^3$ electrons of N as the active electrons and the corresponding orbitals of 4s(Cu), 4p(Cu), 2s(N), and 2p(N) as the active orbitals. So a 6-electron, 8-orbital complete active space multiconfiguration SCF calculation is performed, which is usually abbreviated as CAS(6,8).

The following MRCI calculation is performed by using the CAS(6,8) reference wave functions and estimating the higher-order excitations through the Davidson correction.[17] The excitation type is selected as CISD (single, double excitation configuration interaction), the threshold for the 0th order approximation to the target state is set to be $T_{sel} = 10^{-6}$ Hartree (1 Hartree = 2 Ry = 27.2114 eV), and the second threshold to the 0th order state is set to be $T_{pre} = 10^{-4}$, which is dimensionless and refers to the weight of a given initial reference space.

The scanning step for the PECs is 0.01 nm in a range from 0.10 nm to 0.50 nm. Based on the calculated PECs with the MRCI + Q method, the radial Schrödinger equation of nuclear motion is solved by using the Le Roy provided Level 8.0 program,[18] and the all possible vibrational energy levels are calculated and spectroscopic constants are obtained for each electronic bound state.

3. Results and discussion

3.1. Potential energy curves of the low-lying electronic states of CuN

According to the diatomic molecular structure theory,[19] each electronic state of CuN is related to a specific dissociation limit of Cu + N. For the lowest dissociation limit $Cu(^2S_g)+N(^4S_u)$, only two molecular electronic states are derived in accordance with the Wigner–Witmer rules, where the atomic state ^2S_g of Cu corresponds to $^2\Sigma_g^+$ and the ^4S_u of N corresponds to $^4\Sigma_u^-$ in the $C_{\infty v}$ point group, and the electronic states of CuN can be deduced by the direct product of $^2\Sigma_g^+$ and $^4\Sigma_u^-$, that is, $^2\Sigma_g^+ \otimes {}^4\Sigma_u^- \rightarrow {}^3\Sigma_u^- + {}^5\Sigma_u^-$. Similarly, for the higher $Cu(^2S_g)+N(^2D_u)$ limit, there appear three triplet states and three quintet states, i.e., $^1\Sigma^-$, $^1\Pi$, $^1\Delta$, $^3\Sigma^-$, $^3\Pi$, and $^3\Delta$. Considering the double degeneracy of Π and Δ states, totally twelve PECs are needed to calculate the eight states. In the ORCA program, only D_{2h} and subgroups are supported in the MRCI/CASSCF calculation, the heteronuclear diatomic molecules belonging to the $C_{\infty v}$ point group must be presented with the C_{2v} point group. According to the irreducible presentation relationship between the two point groups, $\Sigma^+ \leftrightarrow A_1$, $\Sigma^- \leftrightarrow A_2$, $\Pi \leftrightarrow B_1 + B_2$, and $\Delta \leftrightarrow A_1 + A_2$, the calculations for the $^1\Sigma^-$, $^1\Pi$, $^1\Delta$, $^3\Sigma^-(2)$, $^3\Pi$, $^3\Delta$, and $^5\Sigma^-$ electronic states of CuN under the $C_{\infty v}$ point group convert into the calculations for the $^1A_1$, $^1A_2(2)$, $^1B_1$, $^1B_2$, $^3A_1$, $^3A_2(3)$, $^3B_1$, $^3B_2$, and $^5A_2$ states under the C_{2v} point group.

Figure 1 displays the calculated PECs of the singlet, triplet, and quintet states labeled with dash curves, solid curves, and empty-circle curve, respectively. The calculated energies for each state are listed in the Supplement attached hereafter (see Appendix A). The inter-nuclear distance changes from 0.1 nm to 0.5 nm. Except for the quintet state $^5\Sigma^-$, the remaining states appear as bound states. The values of adiabatic exciting energy (T_e), equipment bond length (R_e), and dissociation energy (D_e) are listed in Table 1. For comparison, the results of pure MRCI calculation without the Davidson correction are also presented in Table 1, but we only discuss the MRCI + Q results in the following.

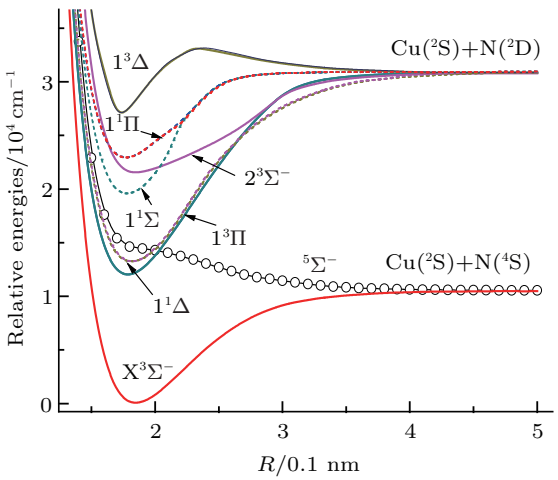


Fig. 1. (color online) Low-lying PECs for the singlet states (dashed lines), triplet states (solid lines), and quintet state (hollow circle pattern line) of CuN calculated with the MRCI + Q/cas(6,8) method and def2-tzvp basis set.

It is clear that the ground state is the $X^3\Sigma^-$ state and the bond length is $R_e = 0.1836$ nm with the lowest energy (−1693.83048) Hartree. We have set this energy to be the reference zero energy level in Fig. 1 and present the PECs with wavenumber units. In the literature, only the ground

state $^3\Sigma^-$ is labeled by X, other states are rarely marked.[9] For convenience of discussion, we sign the electronic excited states as $1^3\Pi$, $1^1\Delta$, $1^1\Sigma^-$, $2^3\Sigma^-$, $1^1\Pi$, and $1^3\Delta$ according to the increase of exciting energy in turn. The first and second excited states, $1^3\Pi$ and $1^1\Delta$, have nearly the same R_e (about 0.178 nm), and their PECs are close and very similar all the way, where their T_e values are at 11912 cm^{-1}(1.477 eV) and 13205 cm^{-1}(1.637 eV), respectively. From Fig. 1, we see all the PECs tend to the two dissociation limits $Cu(^2S_g)+N(^4S_u)$ and $Cu(^2S_g)+N(^2D_u)$ as predicted by the group theory. Daoudi *et al.*[9] calculated the potential energy curves of CuN by the CIPSI method and predicted the first excited state to be $^1\Delta$ with adiabatic exciting energy 1.45 eV. This value is much closer to our calculated value of the $1^3\Pi$ state, where the $1^1\Delta$ state is the second exciting state in our calculation and its exciting energy is slightly (about 0.16 eV) higher than that of the $1^3\Pi$ state. We notice that the asymptote of PEC for the second dissociation limit $Cu(^2S_g)+N(^2D_u)$, calculated by Daoudi,[9] is not well converged compared with our results as shown in Fig. 1.

Table 1. Some important parameters for the low-lying electronic states of CuN calculated with MRCI + Q method.

State	Method	T_0/cm^{-1}*	T_0/eV	R_e/nm	D_e/cm^{-1}	D_e/eV
$X^3\Sigma^-$	MRCI + Q	0.0	0.0	0.1836	10546	1.307
	MRCI	0.	0.	0.1879	8687	1.077
	B3LYP[6]			0.1804		1.89(D_0)
	CCSD(T)[6]			0.1807		1.60(D_0)
	B3LYP[7]			0.1808		1.84
	CIPS I[9]			0.1813		1.20
$1^3\Pi$	MRCI + Q	11912	1.477	0.1776	19008	2.357
	MRCI	11257	1.396	0.1809	17792	2.206
	CIPS I[9]		1.508	0.1784		2.854
$2^3\Sigma^-$	MRCI + Q	21531	2.670	0.1825	9337	1.158
	MRCI	22104	2.740	0.2090	6944	0.861
$1^3\Delta$	MRCI + Q	26489		0.1720	4279	0.530
$1^1\Delta$	MRCI + Q	13205	1.637	0.1799	17729	2.198
	CIPS I[9]		1.452	0.1741		2.467
$1^1\Sigma^-$	MRCI + Q	19491	2.417	0.1764	11514	1.428
$1^1\Pi$	MRCI + Q	22855	2.834	0.1759	8177	1.014
	CIPS I[9]		2.510	0.1729		1.188

* Set the energy (−1693.83048 hartree) of $X^3\Sigma^-$ state at $R_e = 0.1836$ nm as the zero point reference.

3.2. Dipole moment and transition dipole moment

Owing to the ground state of CuN being a triplet state, the allowed electronic transitions between the low-lying excited states and the X state are $2^3\Sigma^-$–$X^3\Sigma^-$ and $1^3\Pi$–$X^3\Sigma^-$. Using the MRCI method to calculate the PECs of CuN, the dipole moments with different bond distances for the $X^3\Sigma^-$, $1^3\Pi$, and $2^3\Sigma^-$ states are computed as shown in Fig. 2.

As shown in Fig. 2, the orientation for the dipole moment points from Cu atom to N atom along the z direction. For the $X^3\Sigma$ state and $1^3\Pi$ state, before the CuN dissociation into neutral atoms after the nuclear distance becomes larger than about 0.4 nm, the dipole moments maintain negative values and reach the extreme values of $D = (-4.19)$ Debye for the $X^3\Sigma$ state at $R = 0.1906$ nm and $D = (-8.44)$ Debye for the $1^3\Pi$ state at $R = 0.2608$ nm, respectively. These results mean that the N atom totally acts as a negative center in the two electronic states. But for the $2^3\Sigma^-$ state, the dipole moment presents an inversion from positive to negative value at $R = 0.222$ nm, the dipole moment reaches a negative extreme value $D = (-3.25)$ Debye at $R = 0.280$ nm. The different electronic states correspond to different electron distributions in the molecular orbitals. The variation of dipole moment with nuclear distance also reflects the effect of the electron configuration. Table 2 gives the main electron configurations for the three states of $X^3\Sigma$, $1^3\Pi$, and $2^3\Sigma^-$ at the nuclear distance when the dipole moments reach their extreme values. The value in the bracket is the weight factor. For the ground state $X^3\Sigma^-$, the main electron configuration is $\delta^2\pi^1\pi^1\sigma^2$, where the unpaired two electrons occupy the π_x and π_y orbital respectively with parallel spin. For the $1^3\Pi$ state, the main configuration is $\delta^2\pi^1\pi^2\sigma^1$ or $\delta^2\pi^2\pi^1\sigma^1$ which correspond to the degenerate $^3\Pi_x$ or $^3\Pi_y$ states. Compared with the ground state configuration, one σ electron is excited to the π orbital, but spin is kept in the same state. For the $2^3\Sigma^-$ state, the main configuration is $\delta^2\pi^1\pi^1\sigma^1\sigma^1$, which means that one σ electron in the ground state is excited to higher another σ orbital.

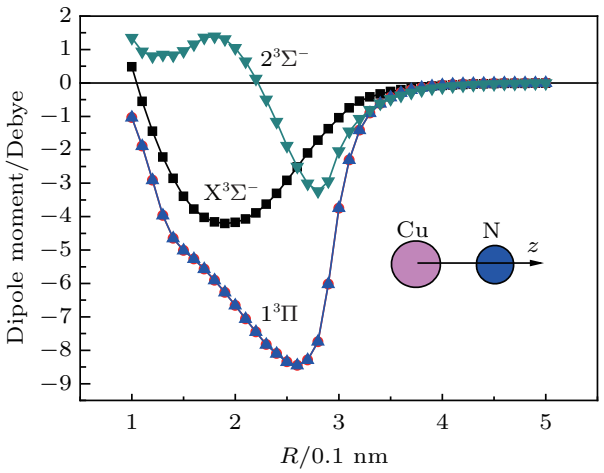


Fig. 2. (color online) Variations of dipole moment with nuclear distance for the three lowest triplet states.

The variations of transition dipole moments of $2^3\Sigma^-$–$X^3\Sigma^-$ and $1^3\Pi$–$X^3\Sigma^-$ with internuclear distance are also computed when scanning the PECs of CuN. As shown in Fig. 3, the dipole moment of the $2^3\Sigma$–$X^3\Sigma^-$ transition is much larger than that of the $1^3\Pi$–$X^3\Sigma^-$ transition. By analyzing the electronic configurations in Table 2, the $2^3\Sigma$–$X^3\Sigma^-$transition corresponds to one σ electron in the low σ orbital excited to another adjacent σ orbital, i.e., $\sigma^2 \rightarrow \sigma^1\sigma^1$, this probability may be much

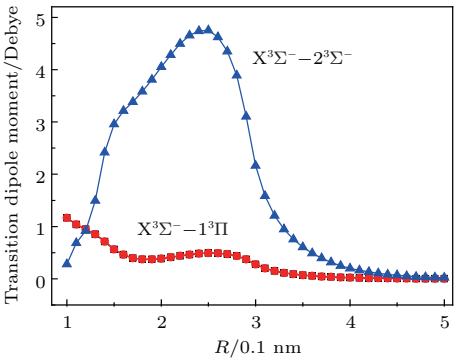


Fig. 3. (color online) Variations of transition dipole moments of $2^3\Sigma^-$–$X^3\Sigma^-$ and $1^3\Pi$–$X^3\Sigma^-$ with internuclear distance.

Table 2. Main electron configurations for the $X^3\Sigma^-$, $1^3\Pi$, and $2^3\Sigma^-$ states at specific nuclear distances.

R/nm	Main configuration		
	$X^3\Sigma^-$	$1^3\Pi$	$2^3\Sigma^-$
0.19	$\delta^2\pi^1\pi^1\sigma^2$ (80%)	$\delta^2\pi^1\pi^2\sigma^1$ (89%)	$\delta^2\pi^1\pi^1\sigma^1\sigma^1$ (77%)
		$\delta^2\pi^2\pi^1\sigma^1$ (89%)	
0.26	$\delta^2\pi^1\pi^1\sigma^2$ (64%)	$\delta^2\pi^1\pi^2\sigma^1$ (88%)	$\delta^2\pi^1\pi^1\sigma^1\sigma^1$ (64%)
	$\delta^2\pi^1\pi^1\sigma^1\sigma^1$ (21%)	$\delta^2\pi^2\pi^1\sigma^1$ (88%)	$\delta^2\pi^1\pi^1\sigma^2$ (23%)
0.28	$\delta^2\sigma^2\pi^1\pi^1$ (59%)	$\delta^2\sigma^1\pi^1\pi^2$ (80%)	$\delta^2\sigma^2\pi^1\pi^1$ (26%)
	$\delta^2\sigma^1\pi^1\pi^1\sigma^1$ (22%)	$\delta^2\sigma^1\pi^2\pi^1$ (80%)	$\delta^2\sigma^1\pi^1\pi^1\sigma^1$ (62%)

larger than that for this electron leaping to the degenerate π orbital, which is correlated with the $1^3\Pi$–$X^3\Sigma^-$ transition. The peak of the transition dipole moment for $2^3\Sigma$–$X^3\Sigma^-$ appears at $R = 0.25$ nm with $D = 4.76$ Debye, but with considering the equilibrium internuclear distance for the ground state $X^3\Sigma^-$, it becomes about $R_e = 0.18$ nm which is far less than the 0.25 nm. This suggests that the possible exciting electronic spectrum cannot achieve the best transition probability.

3.3. Vibrational levels and spectroscopic constants

Based on the MRCI + Q calculated PECs as shown in Fig. 1, all the possible vibrational levels for each bound electronic state of CuN can be obtained by using the first-order semiclassical quantization condition[20] from Wentzel–Kramers–Brillouin (WKB) theory, specifically

$$\left(\frac{2\mu}{\hbar^2}\right)^{1/2}\int_{r_-}^{r_+}\sqrt{E-V(r)}\,\mathrm{d}r = \left(\upsilon+\frac{1}{2}\right)\pi,$$

in which r_- and r_+ are the classical inner and outer turning points for $V(r)$ at the energy E. Using the Level 8.0 computer program, we select the MRCI + Q calculated single point energy of each PEC as the potential energy turning point, and set the integral radial mesh to be 0.0001 nm for solving the one-dimensional Schrödinger equation while the cubic spline interpolation is performed. For the three triplet states $X^3\Sigma^-$, $1^3\Pi$, and $2^3\Sigma^-$, totally 36, 51, and 39 vibrational levels are obtained respectively; while for the three singlet states $1^1\Delta$, $1^1\Sigma^-$, and $1^1\Pi$, there are 54, 28, and 22 vibrational levels respectively. Meanwhile, the rotational constant for each vibrational level is also computed with setting the rotational quantum number J only to be zero. Table 3 shows the first 10 vibrational levels and corresponding rotational constants.

Table 3. Partial vibrational levels and rotational constants (in unit cm^{-1}) of CuN for $X^3\Sigma^-$, $1^3\Pi$, $2^3\Sigma^-$, $1^3\Delta$, $1^1\Delta$, $1^1\Sigma^-$, and $1^1\Pi$ states.

υ	$X^3\Sigma^-$		$1^3\Pi$		$2^3\Sigma^-$		$1^3\Delta$		$1^1\Delta$		$1^1\Sigma^-$		$1^1\Pi$	
	$G(\upsilon)$	B_υ	$G(\upsilon)$	B_υ	$G(\upsilon)$	B_υ	$G(\upsilon)$	B_υ	$G(\upsilon)$	B_υ	$G(\upsilon)$	B_υ	$G(\upsilon)$	B_υ
0	253	0.433	287	0.463	208	0.431	619	0.492	232	0.449	266	0.468	263	0.471
1	747	0.426	852	0.458	578	0.413	1721	0.480	710	0.443	804	0.462	779	0.464
2	1231	0.420	1407	0.453	924	0.402	2595	0.467	1206	0.437	1363	0.459	1283	0.456
3	1707	0.414	1954	0.448	1256	0.390	3334	0.456	1700	0.432	1921	0.453	1770	0.448
4	2173	0.409	2495	0.444	1572	0.379	4002	0.448	2194	0.428	2462	0.446	2231	0.437
5	2628	0.403	3029	0.439	1877	0.370	4618	0.441	2694	0.426	2988	0.442	2656	0.422
6	3072	0.397	3557	0.435	2174	0.362	5185	0.432	3200	0.424	3524	0.442	3042	0.409
7	3506	0.391	4077	0.430	2466	0.355	5688	0.416	3710	0.422	4082	0.444	3418	0.407
8	3928	0.385	4590	0.426	2751	0.348	6101	0.392	4220	0.419	4659	0.445	3811	0.407
9	4340	0.379	5097	0.421	3032	0.342	6451	0.378	4725	0.415	5248	0.445	4217	0.405

Table 4. Spectroscopic constants of the low-lying electronic states of CuN.

State	Method	ω_e/cm^{-1}	$\omega_e x_e$/cm^{-1}	B_e/cm^{-1}	α_e/cm^{-1}
$X^3\Sigma^-$	MRCI + Q	524	6.29	0.426	0.006
	CIPSI[9]	614			
	B3LYP[6]	578			
	CCSD(T)[6]	564			
$1^3\Pi$	MRCI + Q	568	3.30	0.464	0.004
	CIPSI[9]	607			
$2^3\Sigma^-$	MRCI + Q	332	1.72	0.435	0.013
$1^3\Delta$	MRCI + Q	1092	43.4	0.507	0.014
$1^1\Delta$	MRCI + Q	550	3.67	0.452	0.006
	CIPSI[9]	769			
$1^1\Sigma^-$	MRCI + Q	587	3.12	0.471	0.005
$1^1\Pi$	MRCI + Q	497	4.85	0.476	0.008
	CIPSI[9]	558			

Substituting the calculated vibrational level energy into the $G(\upsilon) = \omega_e(\upsilon+1/2) - \omega_e x_e(\upsilon+1/2)^2$ and the rotational constant into $B_\upsilon = B_e - \alpha_e(\upsilon+1/2)$, through the least square fitting, the spectroscopic constants for these bound states are determined as shown in Table 4.

4. Conclusions

In the present study, we calculated the low-lying electronic states of CuN corresponding to the two dissociation limits $Cu(^2S_g) + N(^4S_u)$ and $Cu(^2S_g) + N(^2D_u)$ by making use of the multi-reference configuration interaction (including Davidson correction) method. The potential energy curves

(PECs) of the $X^3\Sigma^-$, $1^3\Pi$, $2^3\Sigma^-$, $^3\Delta$, $1^1\Delta$, $1^1\Sigma^-$, $1^1\Pi$, and $^5\Sigma^-$ in a range of $R = 0.1$ nm$\sim$0.5 nm are obtained. Based on the potential energy curves, all the possible vibrational energy levels, rotational constants, and the corresponding spectroscopic constants for the bound states are obtained, meanwhile, the transition dipole moments from the ground state $X^3\Sigma^-$ to the excited states $1^3\Pi$ and $2^3\Sigma^-$ are calculated and the result indicates that the $2^3\Sigma^-$–$X^3\Sigma^-$ transition keeps a higher transition dipole moment than the $1^3\Pi$–$X^3\Sigma^-$ transition at different nuclear distances.

Appendix A: Supplement material

Table S1. PEC values of CuN calcualted by the MRCI + Q method (in unit cm^{-1}).

R/(0.1 nm)	$X^3\Sigma^-$	$1^3\Pi$	$2^3\Sigma^-$	$1^3\Delta$	$1^1\Delta$	$1^1\Sigma^-$	$1^1\Pi$	R/(0.1 nm)	$X^3\Sigma^-$	$1^3\Pi$	$2^3\Sigma^-$	$1^3\Delta$	$1^1\Delta$	$1^1\Sigma^-$	$1^1\Pi$
1.0	211245	211241	250701	252287	219217	219668	221546	3.0	9168	28781	28751	31790	27567	30805	30827
1.1	127981	127983	157874	160076	134564	133187	135298	3.1	9446	29449	29307	31639	28171	30825	30817
1.2	74009	76851	99184	102088	81350	83103	82734	3.2	9662	29873	29660	31492	28674	30867	30891
1.3	40906	46239	63046	66974	49227	52623	52274	3.3	9839	30150	29920	31376	29089	30888	30908
1.4	21274	28767	41884	47904	31123	35077	36921	3.4	9968	30337	30127	31279	29453	30901	30908
1.5	10065	19155	30525	35539	21224	26217	28642	3.5	10082	30467	30270	31200	29741	30904	30895
1.6	4011	14292	24829	30358	16050	21565	24543	3.6	10166	30558	30388	31136	29961	30908	30911
1.7	1047	12230	22281	26586	13659	19676	22983	3.7	10241	30634	30483	31090	30150	30910	30941
1.8	0	11879	21492	27527	13141	19480	22865	3.8	10302	30698	30554	31060	30266	30916	30898
1.9	94	12533	21599	29133	13436	20123	23489	3.9	10353	30746	30643	31003	30403	30923	30931
2.0	767	13745	21916	30586	14291	21448	24460	4.0	10377	30768	30667	30953	30494	30921	30924
2.1	1777	15302	22367	31873	15577	23094	25335	4.1	10420	30805	30727	30914	30547	30917	30877
2.2	2907	17009	22860	32480	17443	26253	26043	4.2	10438	30819	30747	30883	30625	30912	30871
2.3	4043	18794	23384	33042	19276	27522	27423	4.3	10447	30823	30765	30860	30693	30919	30945
2.4	5131	20543	23956	33224	21054	28759	28662	4.4	10446	30828	30756	30849	30722	30919	30905
2.5	6103	22242	24554	32971	22661	29784	29634	4.5	10461	30831	30777	30847	30786	30925	30922
2.6	6961	23805	25222	32719	23940	30170	30171	4.6	10472	30840	30790	30856	30789	30928	30903
2.7	7687	25289	25972	32449	25112	30490	30481	4.7	10477	30846	30794	30855	30848	30934	30948
2.8	8282	26579	26846	32183	26091	30656	30634	4.8	10479	30850	30802	30860	30845	30938	30945
2.9	8774	27779	27789	31960	26904	30723	30743	4.9	10471	30855	30797	30866	30856	30940	30925
								5.0	10482	30856	30804	30865	30859	30941	30966

References

[1] Veillard A 1991 *Chem. Rev.* **91** 743
[2] Crabtree R H 1985 *Chem. Rev.* **85** 245
[3] Weltner W Jr 1967 *Science* 155
[4] Ruggiero C D, Choi T and Gupta J A 2007 *Appl. Phys. Lett.* **91** 253106
[5] O'Brien L C, Womack K A and O'Brien J J 2012 67*th International Symposium on Molecular Spectroscopy*, Ohio State University, USA
[6] Ferrao L F A, Roberto-Neto O and Machado F B C 2008 *Int. J. Quantum Chem.* **108** 2512
[7] Wu Z J 2006 *J. Comp. Chem.* **27** 267
[8] Xu Y Q, Gao X M and Zhang W J 2007 *Acta Phys. Chim. Sin.* **23** 1075 (in Chinese)
[9] Daoudi A, Benjelloun A T, Flament J P, *et al.* 1999 *J. Mol. Spec.* **194** 8
[10] Neese F 2012 *Wiley Interdisciplinary Reviews: Computational Mol. Sci.* **2** 73
[11] Liu D M and Zhang S D 2012 *Acta Phys. Sin.* **61** 033101 (in Chinese)
[12] Liu C and Zhang S D 2015 *Russ. J. Phys. Chem. A* **89** 1047
[13] Gerard H, Davidson E R and Eisenstein O 2002 *Mol. Phys.* **100** 533
[14] Larsson S 2011 *Int. J. Quantum Chem.* **111** 3424
[15] Weigend F and Ahlrichs R 2005 *Phys. Chem. Chem. Phys.* **7** 3297
[16] Bunge C F, Barrientos J A and Bunge A V 1993 *At. Data Nucl. Data Tables* **53** 113
[17] Langhoff S R and Davidson E R 1974 *Int. J. Quantum Chem.* **8** 61
[18] Le Roy R J 2007 "LEVEL 8.0", A computer program for solving the radial Schrödinger equation for bound and quasibound levels (University of Waterloo, Waterloo, Ontario)
[19] Bernath P F 1995 *Spectra of atomics and molecules* (Oxford University Press)
[20] Schatz G C and Ratner M A 1993 *Quantum Mechanics in Chemistry* (Pretice-Hall, Englewood Cliffs)